HHS Public Access

Author manuscript

Cell Cycle. Author manuscript; available in PMC 2015 April 02.

Published in final edited form as:

Cell Cycle. 2008 September 15; 7(18): 2916–2921.

Color-coded imaging of splenocyte-pancreatic cancer cell interactions in the tumor microenvironment

Michele McElroy[1], **Sharmeela Kaushal**[1], **Michael Bouvet**[1], and **Robert M. Hoffman**[1,2,*]

[1]Department of Surgery; University of California; San Diego, California USA

[2]AntiCancer, Inc.; San Diego, California USA

Abstract

In spite of advances in surgical and medical care, pancreatic cancer remains a leading cause of cancer-related death in the United States. An understanding of cancer-cell interactions with host cells is critical to our ability to develop effective antitumor therapeutics for pancreatic cancer. We report here a color-coded model system for imaging cancer cell interactions with host immune cells within the native pancreas. A human pancreatic cancer cell line engineered to express green fluorescent protein (GFP) in the nucleus and red fluorescent protein (RFP) (DsRed2) in the cytoplasm was orthotopically implanted into the pancreas of a nude mouse. After 10–14 days, red or green fluorescent splenocytes from immune-competent transgenic-mouse donors expressing RFP and GFP, respectively, were delivered systemically to the pancreatic cancer-bearing nude mice. Animals were imaged after splenocyte delivery using high-resolution intravital imaging systems. At 1 day after iv injection red- or green-fluorescent spleen cells were found distributed in lung, liver, spleen and pancreas. By 4 days after cell delivery, however, the immune cells could be clearly imaged surrounding the tumor cells within the pancreas as well as collecting within lymphatic tissues such as lymph nodes and spleen. With the high-resolution intravital imaging afforded by the Olympus IV100 and OV100 systems, the interactions of the dual-colored cancer cells and the red- or green-fluorescent spleen cells could be clearly imaged in this orthotopic pancreatic cancer model. This color-coded in vivo imaging technology offers a novel approach to imaging the interactions of cancer and immune cells in the tumor microenvironment (TME).

Keywords

pancreatic cancer; tumor microenvironment; cancer immunity; GFP; RFP; tumor imaging

Introduction

Although its annual incidence is rare, pancreatic cancer nevertheless represents the 4th leading cause of cancer-related deaths in the United States with the number of cases diagnosed annually roughly equal to its annual mortality rate.[1] Despite recent advances in surgical and medical care, little progress has been made in our treatment for this disease, and

*Correspondence to: AntiCancer, Inc.; 7917 Ostrow Street; San Diego, California 92111 USA; all@anticancer.com.

those diagnosed with this cancer have a 5-year survival rate of less than 5%.[2] The highly lethal nature of this disease is partly explained by its often late stage of presentation but is also due to the aggressive nature of these tumors, which rapidly invade local structures and metastasize by both the hematogenous and lymphatic routes.[3,4]

One of the hallmark features of this cancer is its prominent desmoplastic reaction around the tumor cells.[5,6] In addition to extracellular matrix (ECM) proteins and blood vessels, this fibrous tissue contains abundant stromal cells.[5,7] These stromal cells are believed to play a role not only in the generation of the abundant desmoplastic reaction but may also influence the progression of the disease.[7,8] These recent findings highlight the importance of understanding the impact of the tumor microenvironment on cancer progression.

Both local and distant immune cell interactions with tumor cells may also influence the progression of disease.[9-11] The relationship between host inflammation and cancer development and propagation has been the subject of study since Virchow[12] and remain a poorly understood component of cancer biology. Immune cells have been shown to participate in regulation of angiogenesis,[13,14] tissue remodeling and tumor invasion,[15,16] and may even prepare pre-metastatic sites for eventual tumor cell deposition.[17-19] These findings highlight the importance of elucidating the nuances of the tumor-host interactions which occur within the TME and beyond in order to better understand the mechanisms of tumor growth and metastatsis.

Current methods to image tumor and host interactions have utilized a number of different approaches, each with their own sets of advantages and disadvantages. Noninvasive imaging using magnetic resonance imaging (MRI), positron emission tomography (PET) and single photon emission tomography (SPET) allow whole-body imaging but lack the single-cell and subcellular resolution that can be achieved using intravital microscopy.[20] Likewise, luciferase reporter gene expression can facilitate whole-body imaging of cell population distribution but does not allow imaging of individual cell interactions.[21] Fluorescence imaging technology offers the capacity for multicolor, high-resolution intravital imaging which can be achieved in a living model system.[22,23] We report here a novel in vivo intravital multicolor model system which facilitates the real-time high-resolution imaging of cancer and immune-cell interactions within the microenvironment of the murine pancreas.

Results

In vivo intravital imaging of in situ pancreatic tumors allows for multicolor single-cell resolution imaging of cancer cell interactions with surrounding splenocyte cells. By opening a small abdominal window and exposing the tail of the mouse pancreas with the in situ tumor, we have been able to achieve high-resolution multicolor fluorescence imaging of tumor-immune cell interactions within the living mouse. Rapid image acquisition times allow for multi-filter acquisition of single images as well as in multicolor video acquisition in real time. GFP- or RFP-expressing splenocytes were delivered by intravenous injection to pancreatic tumor-bearing mice, and the interaction of these green fluorescent spleen cells with GFP-RFP pancreatic cancer micrometastases was imaged in vivo using the Olympus OV100 Small Animal Imaging System (Fig. 1).

By varying the filter sets with which the color image is acquired, this imaging technique allows for discrimination between the green (GFP) and red (DsRed2) signals. The GFP long-pass filter set allows the acquisition of both GFP (emission peak 510 nm) and DsRed (emission peak 580 nm) signals simultaneously, facilitating real-time observation of multicolor fluorescent interactions between immune cells and tumor micrometastases. Figures 1A and B; and 2A show several images of GFP-expressing splenocytes interacting in vivo with GFP-RFP pancreatic cancer micrometastases, while Figure 3A shows the interaction of DsRed-expressing spleen cells with micrometastatic GFP-RFP pancreatic tumors. Segregation of the two distinct fluorophore signals by the use of GFP- and RFP-bandpass filter systems allows for discrimination between the two signals and validation of the multicolor imaging (Figs. 2B and C; 3B and C).

In addition, the use of GFP-RFP cancer cells in this model system yields information about cancer cell integrity within the context of these in vivo interactions with immune cells. Cancer cells with intact nucleus and cytoplasm appear to have a red fluorescent cell body with a yellow nucleus due to the overlap of the GFP (green) and DsRed2 (red) signals. Larger groups of cells under low magnification appear yellow to orange under the GFP long-pass filter (Figs. 1A and B; and 2A), whereas individual cells under high magnification appear red and yellow (Fig. 3A). Nonviable cancer cell fragments consisting of either cytoplasm or nuclei can be discriminated under high magnification as the nuclei alone are brightly green under either GFP long-pass or GFP bandpass filter acquisition (Fig. 3A and B) and the cytoplasm alone appears to be a dim orange under GFP long-pass and a dim red under RFP bandpass filter acquisition (Fig. 3A and C).

Using this imaging strategy, intravital imaging of tumor and immune cell interactions can be achieved in real time within the pancreas. Splenocytes from mice engineered to express either DsRed or GFP were delivered to GFP-RFP pancreatic tumor-bearing or naive mice. The distribution of splenocytes in the recipient animals could be imaged in vivo using the Olympus OV100. In the tumor-bearing animals, the fluorescent spleen cells were initially broadly distributed within the animal and especially prevalent in the lungs, liver and spleen. A few fluorescent splenocyte cells could be found within the pancreas at one day post-injection, but the numbers were very low. After four days, however, in vivo imaging of the recipient tumor-bearing pancreas revealed large aggregates of fluorescent immune cells within the pancreatic tissues especially around peritumoral blood vessels. At nine days after systemic delivery of fluorescent splenocytes to tumor-bearing animals, the immune cell aggregates were even more prominent, again predominantly localizing to blood vessels at the periphery of the tumor. After fifteen days, however, the number of fluorescent immune cells within the peritumoral pancreatic tissue had greatly decreased. Animals without pancreatic tumors were likewise given intravenous injections of either GFP- or DsRed-expressing splenocytes. In these control animals, there was minimal aggregation of immune cells within the pancreatic parenchyma at either one, four or fifteen days after splenocyte delivery (data not shown).

Single-cell resolution imaging can be improved down to the subcellular level by using the Olympus IV100 Intravital Scanning Laser Microscope. For complete stabilization of the tissues the animals are sacrificed immediately prior to imaging. Focusing on the interface of

small pancreatic tumors with surrounding GFP-expressing immune cells yields high-resolution subcellular multicolor images of splenocyte homing to the tumor margin within the intact pancreas (Fig. 4). These ultra-high-resolution in situ images show a high density of GFP-expressing splenocytes in the periphery of the GFP-RFP tumors.

Intraperitoneal injection of GFP-expressing splenocytes to GFP-RFP pancreatic tumor-bearing mice likewise yielded immune-cell homing to peritumoral pancreatic tissues within four days of splenocyte injection (Fig. 5). In vivo intravital imaging using the Olympus OV100 at day one after injection demonstrated very few fluorescent immune cells within the pancreas. However, by day four there were numerous collections of green-fluorescent splenocytes within pancreatic tissue adjacent to the tumor. The number of peritumoral fluorescent splenocytes increased up until day nine and again was diminished by day fifteen. The immune cells in these animals were sometimes found immediately adjacent to blood vessels (Fig. 5A). Again, in non-tumor-bearing animals, there were very few GFP-expressing immune cells found in the pancreas at any time point (data not shown). Higher resolution imaging with subcellular detail was obtained using the Olympus IV100 Scanning Laser Microscope System. Evaluation of the tumor-host interface using this technology yielded detailed images of GFP-expressing immune cell interactions with the primary tumor itself (Fig. 5B).

Discussion

The tumor microenvironment is a fundamental part of cancer growth and progression. We describe here a model system which allows multicolor, intravital in vivo evaluation of pancreatic cancer cells and immune cells within the native environment of the pancreas. Splenocytes from immune-competent mice expressing wither GFP or DsRed homed to the orthotopic pancreatic tumors within 4 days of systemic administration. In non-tumor bearing animals, there were very few splenocytes present within the pancreas at any time point. Fluorescent splenocytes could also be imaged interacting with peritumoral micrometastases within the pancreas in living mice. The use of GFP-RFP cancer cells expressing GFP in the nucleus and DsRed2 in the cytoplasm allowed the cancer cells to be distinguished from the fluorescent immune cells as well as from cancer cell fragments.

Previous imaging techniques which have imaged tumor-host interactions within orthotopic model systems have largely relied on low-resolution noninvasive imaging with or without additional contrast agents to enhance imaging sensitivity.[20,21,24] A few more recent model systems have been developed which utilize fluorescence intravital imaging technology to evaluate tumor-host interactions. Lewis et al.,[25] report the use of fluorescent-labeled cowpea mosaic virus for in vivo vascular imaging in both mouse and chick embryo models with a signal duration of approximately 72 hours. Swirski et al.,[22] utilized mammalian leukocytes transiently labeled with a near-infrared probe to track immune responses using both whole-body and intravital imaging. In this model, the ex-vivo labeled immune cells maintain their fluorescence signal for 3 days in vivo.[22] Our group has recently utilized stably transduced tumor cell lines which express GFP in the nucleus and DsRed2 in the cytoplasm in the context of GFP-expressing host tissues to image tumor-host interactions in vivo.[23,26,27] Fluorescent-protein-based imaging has the advantage of allowing multicolor in vivo imaging

in the context of cells which stably express fluorophore, facilitating repeated imaging over time in the same animal.[28-33] None of these previously published models, however, have evaluated tumor-host interactions within the pancreatic cancer microenvironment using in vivo multicolor intravital imaging.

We present here high-resolution imaging of tumor-immune cell interactions within the native microenvironment of pancreatic cancer. This novel imaging model system facilitates the observation of immune cell interactions with pancreatic cancer cells within the orthotopic tumor microenvironment over time. In this orthotopic model of pancreatic cancer, we are able to visualize the homing of fluorescent spleen cells to the tumor-bearing pancreas and to micrometastatic lesions within the pancreatic parenchyma. This technique achieves high-resolution imaging of cancer cell and immune cell interactions within the pancreatic cancer microenvironment in the living animal, improving our ability to study tumor-host interactions in vivo.

Materials and Methods

Cell culture

The human pancreatic cancer cell line XPA1 was a gift from Dr. Anirban Maitra at Johns Hopkins University. Cells were maintained in RPMI 1640 media supplemented with 10% fetal bovine serum (FBS) and 2 mM glutamine from Gibco-BRL, Life Technologies, Inc., (Grand Island, NY). All media were supplemented with penicillin/streptomycin (Gibco-BRL), L-glutamine (Gibco-BRL), MEM nonessential amino acids (Gibco-BRL), sodium bicarbonate (Cellgro, Herndon VA), and sodium pyruvate (Gibco-BRL). All cell lines were cultured at 37°C with 5% CO_2.

Production of the histone H2B-GFP vector

The histone *H2B-GFP* fusion gene was inserted at the *Hin*dIII/*Cal*I site of the pLHCX plasmid (Clontech Laboratories, Inc., Mountain View CA) containing the hygromycin resistance gene. Plasmids were transfected into PT67 packaging cells cultured in DMEM (Gibco-BRL) with 10% FBS using the LipofectAMINE system (Gibco-BRL). PT67 cells at 70% confluence were incubated with the LipofectAMINE reagent and the pLHCX-H2B-GFP plasmid for 18 hours, at which point the medium was replenished. Forty-eight hours later the cells were examined by fluorescence microscopy and vector production was accomplished via growth in PT67 packaging cells cultured in the presence of 200–400 μg/mL hygromycin for 7 days.[26,32,33]

Production of the DsRed2 retroviral vector

The *Hin*dIII/*Not*I fragment of pDsRed2 (Clontech Laboratories, Inc.,) was inserted into the *Hin*dIII/*Not*I site of the pLNCX2 plasmid (Clontech Laboratories, Inc.,) containing the neomycin resistance gene to produce the pLNCX2-DsRed2 plasmid. Plasmids were transfected into PT67 packaging cells as described above using the LipofectAMINE system (Gibco-BRL). Vector production was accomplished via growth in PT67 packaging cells cultured in the presence of 200–1000 μg/mL G418 for 7 days.[26,32,33]

Production of a GFP-RFP pancreatic cancer cell line

XPA1 cells were first stably transduced to express DsRed2 in the cytoplasm by incubation with supernatant from PT67 cells transfected with the pLNCX2 plasmid containing the pDsRed2 gene for 72 hours. After transduction, the cells were harvested and subcultured in selective media containing G418 increased in stepwise fashion from 200 to 800 mg/mL. The cells were then incubated for 72 hours in supernatant from PT67 cells transfected with the pLHCX plasmid containing the H2B-GFP fusion gene. After 72 hours the cells were grown in selective medium containing hygromycin. The level of hygromycin was increased in a stepwise fashion up to 400 mg/mL. The resultant XPA1-GFP-RFP cells expressed DsRed2 in the cytoplasm and GFP in the nucleus.[26,27,32,33]

Animal care

Athymic *nu/nu* nude mice and C57/B6 mice engineered to express either dsRed or GFP fluorescent proteins were maintained in a barrier facility on high efficiency particulate air (HEPA)-filtered racks. The animals were fed with autoclaved laboratory rodent diet (Teckland LM-485; Western Research Products, Orange, CA). All surgical procedures and imaging were performed with the animals anesthetized by intramuscular injection of 0.02 mL of a solution of 50% ketamine, 38% xylazine and 12% acepromazine maleate. All animal studies were conducted in accordance with the principles and procedures outlined in the NIH Guide for the Care and Use of Animals.

Establishing dual-colored orthotopic pancreatic tumors

Orthotopic human pancreatic cancer xenografts from the pancreatic cancer cell line XPA1-GFP-RFP were established in nude mice by orthotopic implantation. Four-to-six week old female *nu/nu* mice were anesthetized as described, and a small transverse incision was then made in the left lateral flank through the skin and peritoneum. The tail of the pancreas was exposed and 1×10^6 XPA1-GFP-RFP cells in 30 μL final volume were injected into the pancreatic tail. The pancreas was then returned to the abdomen, and the peritoneum and skin were closed using 6–0 polysorb surgical suture (US Surgical). Tumors were allowed to grow for 10–14 days prior to the injection of fluorescent splenocytes.

Transgenic GFP and DsRed mice

Transgenic C57/B6-GFP mice were obtained from Prof. Masaru Okabe from the Research Institute for Microbial Diseases, Osaka University, Osaka, Japan.[23] These mice express GFP under the control of the chicken β-actin promoter and cytomegalovirus enhancer. All tissues in this animal with the exception of erythrocytes and hair express GFP. Transgenic DsRed mice were purchased from Jackson Laboratories. These mice express DsRed under the control of the chicken β-actin promoter and cytomegalovirus enhancer.[34] All tissues with the exception of hair and erythrocytes express DsRed in these animals. Transgenic DsRed mice were crossed with C57/B6 mice to generate transgenic C57/B6-DsRed mice.

Splenocyte harvest

C57/B6 mice engineered to express either DsRed or GFP in all tissues were used for splenocyte acquisition. Animals were euthanized, and their spleens were harvested under

sterile conditions. The splenic tissue was first sectioned into pieces using sterile surgical instruments and then gently compressed between two slides to release the individual cells. The cells were passed through an 80 μm filter and pelleted. The spleen cells were then resuspended in 1 mL/spleen of BD PharmLyse Buffer (BD Biosystems) and kept at room temperature for 1 minute. RPMI with 10% FBS was added to dilute the solution 1:10, and the cells were again spun down. The final pellet was resuspended in serum-free media and passed again through an 80 μm filter. Approximately 5×10^7 splenocytes were used for each tumor-bearing or control animal.

Splenocyte injection

Both tumor-bearing and non-tumor-bearing (control) mice were given a single injection of DsRed or GFP-expressing splenocytes in 100 μL volume at a final cell concentration of 5×10^8 cells/mL. Injections were given either intravenously (via tail vein injection) or intraperitoneally.

Animal imaging

Mice were imaged using either the Olympus OV100 Small Animal Imaging System (Olympus Corp., Tokyo, Japan), containing an MT-20 light source (Olympus Biosystems Planegg, Germany) and DP70 CCD camera (Olympus Corp., Tokyo, Japan), or the Olympus IV100 Intravital Scanning Laser Microscope (Olympus Corp., Tokyo, Japan). For imaging on the OV100, animals were deeply anesthetized as described. For imaging on the IV100, animals were sacrificed immediately prior to image acquisition. In each case, the pancreas was exposed via a midline abdominal incision at the time of imaging. All images were analyzed using Image-J (National Institute of Health Bethesda, MD) and were processed for contrast and brightness with the use of Photoshop Element-4 (Adobe Systems Inc., San Jose, CA).

Acknowledgements

This work was supported in part by grants Cancer Therapeutics Training Program (TE CA 121938), National Institute of Health (CA 109949-03), American Cancer Society (RSG-05-037-01-CCE) (M.B.) and National Cancer Institute (CA 099258 and CA 103563) (AntiCancer Inc.).

Abbreviations

TME	tumor microenvironment
IV	intravenous
IP	intraperitoneal
PET	positron emission tomography
SPET	single photon emission tomography
MRI	magnetic resonance imaging

References

1. Ries, L.; Melbert, D.; Krapcho, M.; Stinchcomb, D.; Howlader, N.; Horner, M.; Mariotto, A.; Miller, B.; Feuer, E.; Altekruse, S.; Lewis, D.; Clegg, L.; Eisner, M.; Reichman, M.; Edwards, B. SEER Surveillance Epidemiology and End Results. Bethesda, MD: 2008. SEER Cancer Statistics Review, 1975–2005, National Cancer Institute; p. 8based on November 2007 SEER data submission, posted to the SEER web site
2. Wray CJ, Ahmad SA, Matthews JB, Lowy AM. Surgery for pancreatic cancer: recent controversies and current practice. Gastroenterology. 2005; 128:1626–41. [PubMed: 15887155]
3. Kamisawa T, Isawa T, Koike M, Tsuruta K, Okamoto A. Hematogenous metastases of pancreatic ductal carcinoma. Pancreas. 1995; 11:345–9. [PubMed: 8532650]
4. Pawlik TM, Gleisner AL, Cameron JL, Winter JM, Assumpcao L, Lillemoe KD, Wolfgang C, Hruban RH, Schulick RD, Yeo CJ, Choti MA. Prognostic relevance of lymph node ratio following pancreaticoduodenectomy for pancreatic cancer. Surgery. 2007; 141:610–8. [PubMed: 17462460]
5. Apte MV, Park S, Phillips PA, Santucci N, Goldstein D, Kumar RK, Ramm GA, Buchler M, Friess H, McCarroll JA, Keogh G, Merrett N, Pirola R, Wilson JS. Desmoplastic reaction in pancreatic cancer: role of pancreatic stellate cells. Pancreas. 2004; 29:179–87. [PubMed: 15367883]
6. Bachem MG, Schunemann M, Ramadani M, Siech M, Beger H, Buck A, Zhou S, Schmid-Kotsas A, Adler G. Pancreatic carcinoma cells induce fibrosis by stimulating proliferation and matrix synthesis of stellate cells. Gastroenterology. 2005; 128:907–21. [PubMed: 15825074]
7. Vonlaufen A, Joshi S, Qu C, Phillips PA, Xu Z, Parker NR, Toi CS, Pirola RC, Wilson JS, Goldstein D, Apte MV. Pancreatic stellate cells: partners in crime with pancreatic cancer cells. Cancer Res. 2008; 68:2085–93. [PubMed: 18381413]
8. Hwang RF, Moore T, Arumugam T, Ramachandran V, Amos KD, Rivera A, Ji B, Evans DB, Logsdon CD. Cancer-associated stromal fibroblasts promote pancreatic tumor progression. Cancer Res. 2008; 68:918–26. [PubMed: 18245495]
9. Balkwill F, Coussens LM. Cancer: an inflammatory link. Nature. 2004; 431:405–6. [PubMed: 15385993]
10. DeNardo DG, Johansson M, Coussens LM. Immune cells as mediators of solid tumor metastasis. Cancer Metastasis Rev. 2008; 27:11–8. [PubMed: 18066650]
11. Karin M, Greten FR. NFkappaB: linking inflammation and immunity to cancer development and progression. Nature Rev Immunol. 2005; 5:749–59. [PubMed: 16175180]
12. Coussens LM, Werb Z. Inflammation and cancer. Nature. 2002; 420:860–7. [PubMed: 12490959]
13. Bergers G, Brekken R, McMahon G, Vu TH, Itoh T, Tamaki K, Tanzawa K, Thorpe P, Itohara S, Werb Z, Hanahan D. Matrix metalloproteinase-9 triggers the angiogenic switch during carcinogenesis. Nature Cell Biol. 2000; 2:737–44. [PubMed: 11025665]
14. Coussens LM, Raymond WW, Bergers G, Laig-Webster M, Behrendtsen O, Werb Z, Caughey GH, Hanahan D. Inflammatory mast cells upregulate angiogenesis during squamous epithelial carcinogenesis. Genes Dev. 1999; 13:1382–97. [PubMed: 10364156]
15. Balkwill F, Charles KA, Mantovani A. Smoldering and polarized inflammation in the initiation and promotion of malignant disease. Cancer Cell. 2005; 7:211–7. [PubMed: 15766659]
16. Condeelis J, Pollard JW. Macrophages: obligate partners for tumor cell migration, invasion and metastasis. Cell. 2006; 124:263–6. [PubMed: 16439202]
17. Acuff HB, Carter KJ, Fingleton B, Gorden DL, Matrisian LM. Matrix metalloproteinase-9 from bone marrow-derived cells contributes to survival but not growth of tumor cells in the lung microenvironment. Cancer Res. 2006; 66:259–66. [PubMed: 16397239]
18. Hiratsuka S, Watanabe A, Aburatani H, Maru Y. Tumour-mediated upregulation of chemoattractants and recruitment of myeloid cells predetermines lung metastasis. Nature Cell Biol. 2006; 8:1369–75. [PubMed: 17128264]
19. Kaplan RN, Psaila B, Lyden D. Bone marrow cells in the ‘pre-metastatic niche’: within bone and beyond. Cancer Metastasis Rev. 2006; 25:521–9. [PubMed: 17186383]
20. Ottobrini L, Lucignani G, Clerici M, Rescigno M. Assessing cell trafficking by noninvasive imaging techniques: applications in experimental tumor immunology. Q J Nucl Med Mol Imaging. 2005; 49:361–6. [PubMed: 16407819]

21. Klopp AH, Spaeth EL, Dembinski JL, Woodward WA, Munshi A, Meyn RE, Cox JD, Andreeff M, Marini FC. Tumor irradiation increases the recruitment of circulating mesenchymal stem cells into the tumor microenvironment. Cancer Res. 2007; 67:11687–95. [PubMed: 18089798]
22. Swirski FK, Berger CR, Figueiredo JL, Mempel TR, von Andrian UH, Pittet MJ, Weissleder R. A near-infrared cell tracker reagent for multiscopic in vivo imaging and quantification of leukocyte immune responses. PLoS ONE. 2007; 2:e1075. [PubMed: 17957257]
23. Yang M, Jiang P, Hoffman RM. Whole-body subcellular multicolor imaging of tumor-host interaction and drug response in real time. Cancer Res. 2007; 67:5195–200. [PubMed: 17545599]
24. Pahernik S, Griebel J, Botzlar A, Gneiting T, Brandl M, Dellian M, Goetz AE. Quantitative imaging of tumour blood flow by contrast-enhanced magnetic resonance imaging. Br J Cancer. 2001; 85:1655–63. [PubMed: 11742483]
25. Lewis JD, Destito G, Zijlstra A, Gonzalez MJ, Quigley JP, Manchester M, Stuhlmann H. Viral nanoparticles as tools for intravital vascular imaging. Nature Med. 2006; 12:354–60. [PubMed: 16501571]
26. Hoffman RM, Yang M. Color-coded fluorescence imaging of tumor-host interactions. Nature Protoc. 2006; 1:928–35. [PubMed: 17406326]
27. Jiang P, Yamauchi K, Yang M, Tsuji K, Xu M, Maitra A, Bouvet M, Hoffman RM. Tumor cells genetically labeled with GFP in the nucleus and RFP in the cytoplasm for imaging cellular dynamics. Cell Cycle. 2006; 5:1198–201. [PubMed: 16760659]
28. Glinsky GV, Glinskii AB, Berezovskaya O, Smith BA, Jiang P, Li XM, Yang M, Hoffman RM. Dual-color-coded imaging of viable circulating prostate carcinoma cells reveals genetic exchange between tumor cells in vivo, contributing to highly metastatic phenotypes. Cell Cycle. 2006; 5:191–7. [PubMed: 16357534]
29. Berezovska OP, Glinskii AB, Yang Z, Li XM, Hoffman RM, Glinsky GV. Essential role for activation of the Polycomb Group (PcG) protein chromatin silencing pathway in metastatic prostate cancer. Cell Cycle. 2006; 5:1886–901. [PubMed: 16963837]
30. Yamauchi K, Yang M, Hayashi K, Jiang P, Yamamoto N, Tsuchiya H, Tomita K, Moossa AR, Bouvet M, Hoffman RM. Imaging of nucleolar dynamics during the cell cycle of cancer cells in live mice. Cell Cycle. 2007; 6:2706–8. [PubMed: 17912040]
31. Hoffman RM. The multiple uses of fluorescent proteins to visualize cancer in vivo. Nature Rev Cancer. 2005; 5:796–806. [PubMed: 16195751]
32. Hoffman RM, Yang M. Subcellular imaging in the live mouse. Nature Protoc. 2006; 1:775–82. [PubMed: 17406307]
33. Hoffman RM, Yang M. Whole-body imaging with fluorescent proteins. Nature Protoc. 2006; 1:1429–38. [PubMed: 17406431]
34. Vintersten K, Monetti C, Gertsenstein M, Zhang P, Laszlo L, Biechele S, Nagy A. Mouse in red: red fluorescent protein expression in mouse ES cells, embryos, and adult animals. Genesis. 2004; 40:241–6. [PubMed: 15593332]

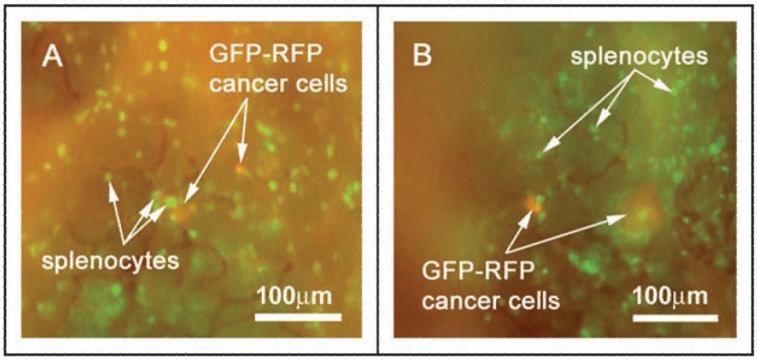

Figure 1.

Intravital imaging of the orthotopic tumor microenvironment using the OV100 demonstrates GFP-expressing splenocyte interactions with GFP-RFP micrometastases within the pancreas. GFP-RFP tumor-bearing animals were given a single i.v. injection of GFP-expressing splenocytes. The animals were imaged at 9 days after splenocyte injection. In vivo image acquisition with the GFP longpass filter allows simultaneous signal acquisition from the GFP-RFP micrometastases adjacent to the primary tumor as well as the GFP-expressing splenocytes within the surrounding pancreatic tissue. High resolution images (A and B) can be acquired in vivo due to the short image acquisition times. Imaging was with the Olympus OV100

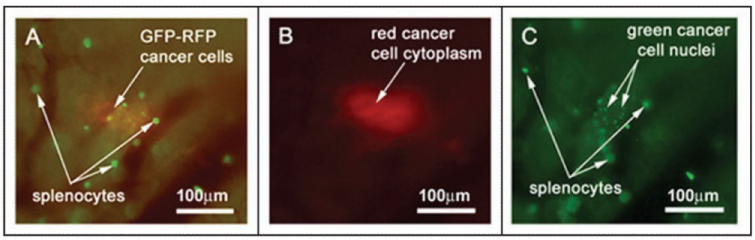

Figure 2.

Multicolor imaging using different fluorescence emission filters allows for discrimination between cancer cells and GFP-expressing splenocytes within the native pancreas in vivo. GFP-RFP tumor-bearing animals were given a single i.v. injection of GFP-expressing splenocytes. The animals were imaged at 9 days after splenocyte injection. (A) Use of the GFP long-pass filter allows visualization of both green and red fluorescent signals from the cancer cells as well as the isolated green signal from the splenocytes. (B) The RFP narrow-band filter allows discrimination of the DsRed2 signal from the tumor cell cytoplasm. (C) The GFP narrow-band filter shows GFP signals from the cancer-cell nuclei as well as GFP-expressing splenocytes. Imaging was with the Olympus OV100.

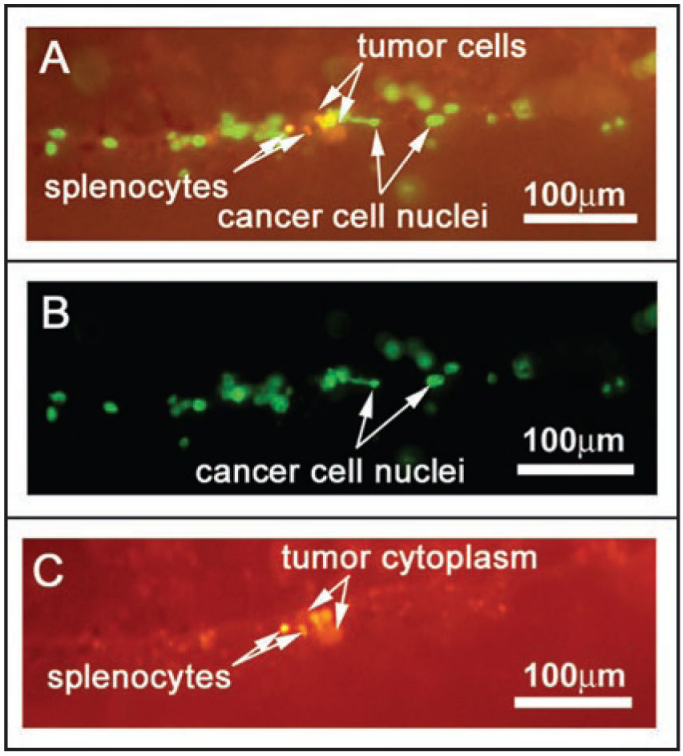

Figure 3.

Multicolor imaging using different fluorescence emission filters allows for discrimination between cancer cells and DsRed-expressing splenocytes within the native pancreas in vivo. GFP-RFP tumor-bearing animals were given a single i.v. injection of DsRed-expressing splenocytes. The animals were imaged at 9 days after splenocyte injection. (A) Use of the GFP longpass filter allows visualization of both green and red fluorescent signal from the cancer cells as well as the isolated red signal from the splenocytes. (B) The GFP narrow-band filter allows imaging of the GFP signal from the cancer cell nuclei. Cancer cell fragments can be discriminated from whole cells based on morphology. (C) The RFP narrow-band filter shows DsRed2 signals from the cancer-cell cytoplasm as well as DsRed expressing splenocytes. Imaging was with the Olympus OV100

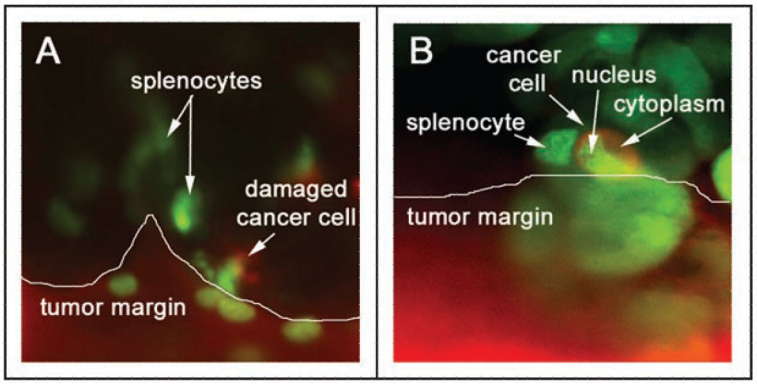

Figure 4.

IV100 Imaging of GFP-expressing splenocyte interactions with the GFP-RFP tumor margin. GFP-RFP tumor-bearing animals were given a single i.v. injection of GFP-expressing splenocytes. The animals were imaged at 9 days after splenocyte injection. The scanning laser microscope system allows high resolution imaging of single cells within the pancreatic microenvironment. (A) The GFP-RFP tumor margin with red fluorescent cytoplasm and green fluorescent nuclei are shown with adjacent green fluorescent spleen cells and damaged GFP-RFP cancer cells in the peritumoral tissue. (B) High-resolution imaging allows for observation of both cancer cell-immune cell interactions as well as individual tumor cell morphology. All images taken with IV100 20x objective.

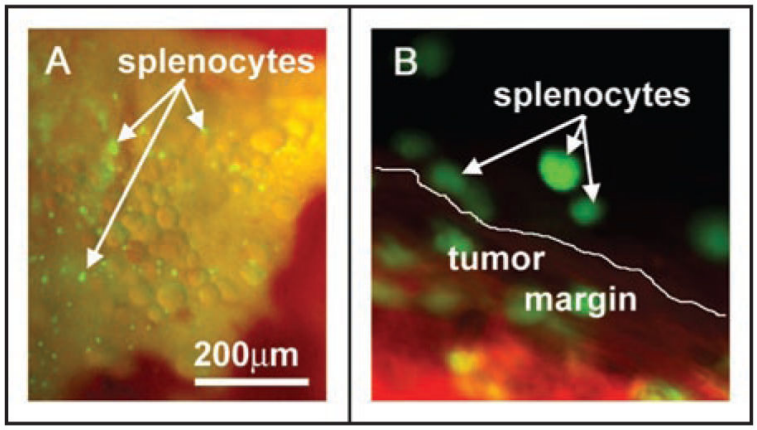

Figure 5.

GFP-expressing splenocytes imaged within the peritumoral pancreatic tissue after IP injection. Murine pancreatic tissue with orthotopic GFP-RFP tumors was imaged 9 days after IP injection of GFP-expressing splenocytes. Animals were imaged on the Olympus OV100 Small Animal Imaging System (A) and the Olympus IV100 Scanning Laser Small Animal Imaging System (B). (A) Pancreatic tissue adjacent to the tumor shows numerous green fluorescent splenocytes at 9 days post-injection as imaged on the OV100 using the GFP long-pass filter. (B) GFP-expressing spleen cells can be distinguished from the GFP-RFP tumor margin and imaged with subcellular resolution using the IV100 (image taken with 20x objective).